



WHITE PAPER: APELC DIAGNOSTICS & MEASUREMENT METHODS

Author: Matt Lara

Applied Physical Electronics L.C. (APELC) designs, manufacturers, and tests a wide array of high-power RF devices. In doing so, APELC has aggregated the working knowledge and hardware necessary to capture and analyze the various signals produced by each device. The following document outlines the types of signals generated by APELC/APELC customer hardware, and the tools used to acquire and analyze each of the different waveforms.

1. Characterization of Measured Signals

1.1 Ultra-wideband

Although several definitions of Ultra-wideband exist, one accepted definition produced by the Defense Advanced Research Project Agency (DARPA) in their 1990 *Assessment of Ultra-Wideband Radar*, states that “Ultra-wideband” refers to a signal “whose fractional bandwidth is greater than .25, regardless of the center frequency of the signal time-bandwidth product.”

[REF1] In practice however, an ultra-wideband signal can be more generally characterized by its time-domain waveform, as a signal which at the source is a double-exponential waveform, and radiated, is the first derivative of the double-exponential, as illustrated in Figure 1a. The Fast-Fourier Transform (FFT) of such a signal (Figure 1b) exhibits a high frequency component which falls off at a 3-dB point corresponding to the rising edge of the signal. The remainder, and majority of the energy contained in the signal, is a result of the trailing edge of the time-domain waveform.

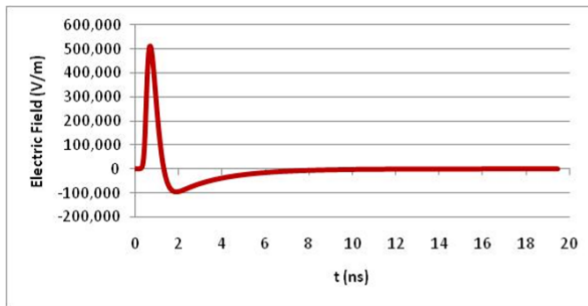
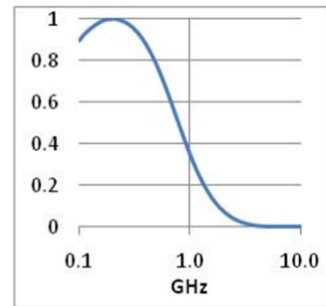


Figure 1 Ultra-wideband signal: a.) Time-domain



b.) Frequency-domain

[REF2] provides an example of such a system, in which a Marx generator directly drives a linear half-TEM horn antenna. The source is placed 100 meters away from a matched receiving antenna, and both are raised 10 meters off the ground to reduce reflections from the ground.

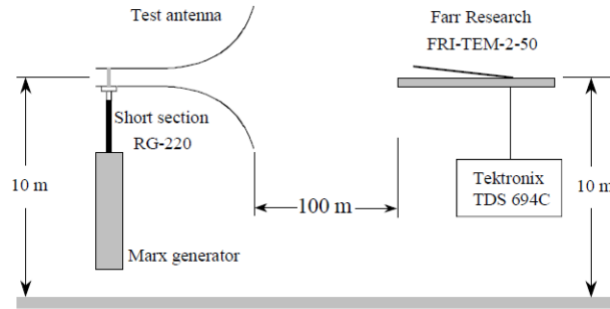


Figure 2 Marx generator-driven linear half-TEM antenna setup

The Marx generator produces a double-exponential pulse with a rise-time of 250 ps. Using the following relation for rise-time and frequency [REF3], high-frequency content up to 1.4 GHz is expected and then observed in Figure 3.

$$f = \frac{.35}{t_{rise}}$$

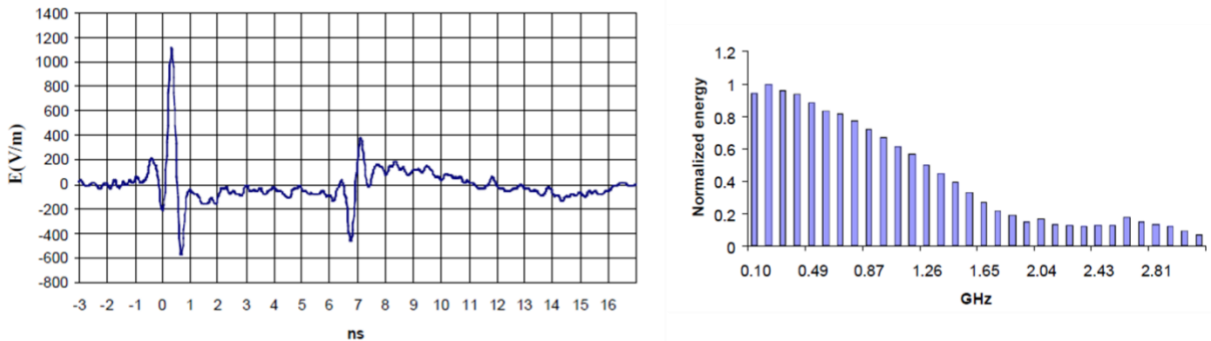


Figure 3 Time and Frequency-Domain plots for the Marx-driven linear half-TEM

1.2 Wideband (Mesoband)

In continuing with the definition stated in [REF1], a wideband signal is one whose fractional bandwidth ranges from 1 to 25%. Again, the time-domain waveform provides a more practical definition of a wideband signal for the purposes of this document. Pictured in Figure 4a., the wideband signal is most often an exponentially damped sinewave. This results in an FFT (Figure 4b.) with a clearly defined center frequency, and considerable frequency content at both the upper and lower end of the band.

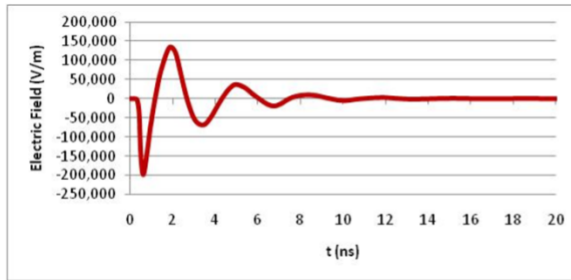
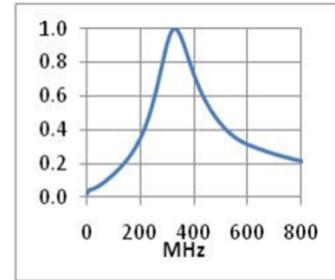


Figure 4 Wideband signal: a.) Time-domain



b.) Frequency-domain

The most commonly tested source at APELC is a resonator-driven fat-dipole. This type of radiator produces a signal ten's of nanoseconds in duration with a center frequency in the tens to hundreds of MHz, very similar to the one shown in Figure 4.

An example of such a system would be the APELC RFSC-400 shown below in Figure 5.



Figure 5 APELC RFSC-400 MHz high-power wideband suitcase system

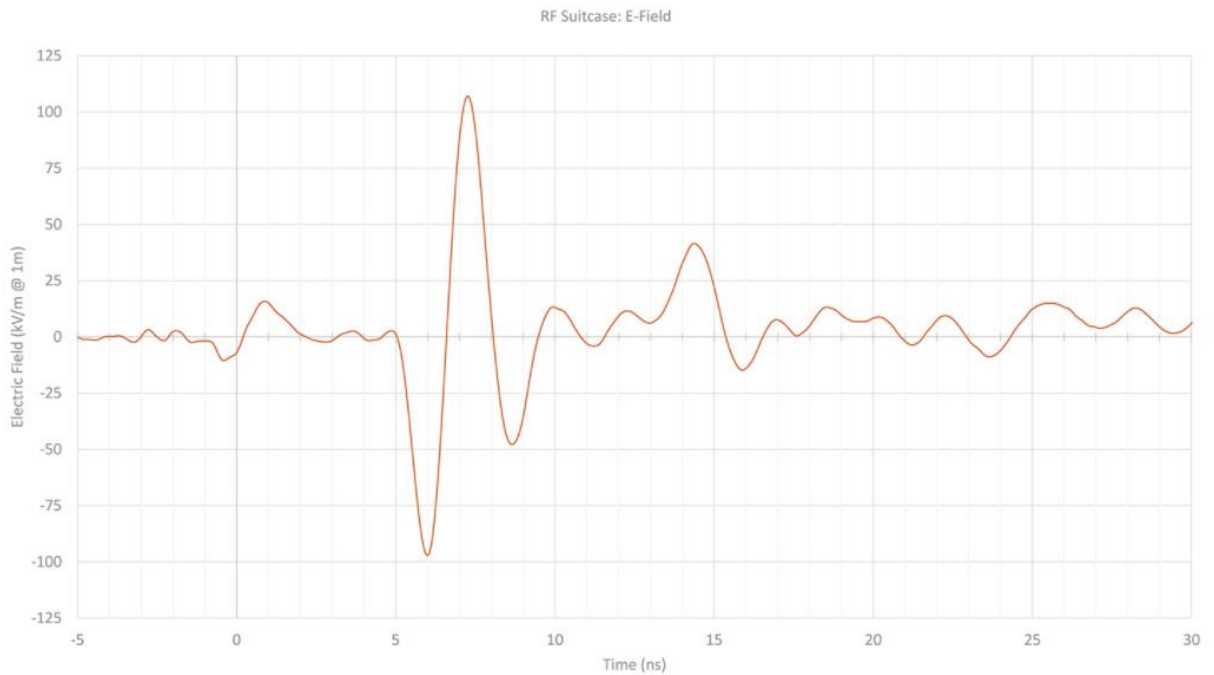


Figure 6 APELC RFSC-400 MHz electric field strength at 1m

1.3 Narrowband

While a narrowband source can be Continuous-Wave (CW), in the field of directed-energy such sources most often generate pulses lasting hundreds of nanoseconds in duration. As is evident in Figure 7 the narrowband signal contains hundreds or thousands of cycles, resulting in a fractional bandwidth <1%.

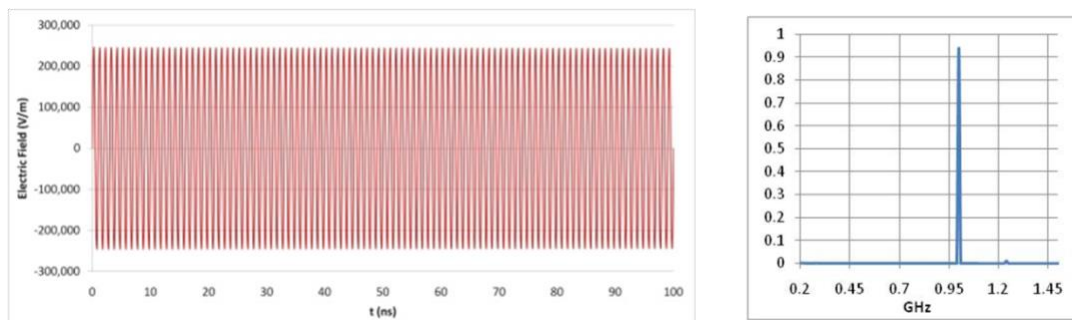


Figure 7 Narrowband signal a.) Time-domain

b.) Frequency-domain

An example of such a system manufactured and tested at APELC is the Virtual-cathode Oscillator or Vircator. This type of source produces high-power microwave radiation by generating an electron beam which exceeds the space-charge-limiting current, and in doing so producing a dense region of charge known as a “virtual cathode”. The change in position of the virtual cathode, as well as the repelling of the incoming electrons by the space charge, results in the generation of microwave energy [REF4].

2. Sensors/Probes

As mentioned in the previous section, two out of three of the classifications of high-power RF/microwave systems manufactured and tested by APELC have a bandwidth which can be considered wideband or ultra-wideband. Specifically, the dipole radiators commonly tested at APELC have a percentage bandwidth of 25% or greater. Therefore, the receiving antenna must also be a wideband/ultra-wideband device to accurately capture the signal. APELC uses two different types of receiving antennas to capture signals radiated by pulsed, high-power RF systems: The double-ridge horn, and the D-dot electric field sensor.

Initially, the double-ridge horn was used for far-field measurements, and the D-dot sensor was used strictly as a field probe for bounded wave EMP simulators (MIL-STD 461G/RS-105). However, continued use of the horn antenna revealed that changes of >2 dB in the antenna factor, for a change of 10 MHz in frequency, yielded a high degree of uncertainty in the measurement for a wideband radiator. Furthermore, the high gain of the antenna resulted in a relatively high voltage at the output port of the antenna, consequently increasing the incidence of failure related to electrical breakdown of cabling and attenuators. As a result, the D-dot sensor was adopted for far field measurements of wideband/ultra-wideband devices, due to its flat frequency response and small receiving area (lower voltages at the output port). The double-ridge horn continues to be used as a diagnostic for the measurement of narrowband devices, for receiving low power signals in remote sensing applications, and for gain characterization of other antennas.

2.1 A.H. Systems SAS-570 Double Ridge Guide Horn Antenna

The Double-Ridge Guide Horn (DRGH) antenna is a horn antenna loaded with a central ridge which increases the bandwidth of the device by lowering the cutoff frequency of the dominant mode [REF5]. The SAS-570 antenna (Figure 8) used by APELC covers a frequency range of 170 MHz to 3 GHz, and is used for measuring both narrow and wideband, linearly polarized signals. Specifications for the antenna are listed in Table 1 [REF6].



Figure 8 A.H. Systems, SAS-570 double-ridge horn antenna

Table 1 SAS-570 Specifications

Frequency Range	.170-3	GHz
Antenna Factor (1 Meter)	11 to 33	dB
Gain	0 to 10.9	dBi
Maximum Continuous Power	800	Watts
Impedance	50	Ohms
Max Radiated Field	200	V/m
Connector	N-Type, female	
Mounting Base	¼ - 20 Thread, female	

While the SAS-570 has been replaced by the Prodyn D-dot sensor for far field measurement of most high-power RF radiators, the antenna is still very useful in characterizing an antenna with an unknown gain. APELC commonly uses such a configuration to determine the gain of a newly fabricated helical antenna. Figure 9 demonstrates a typical setup for a two-antenna gain measurement, in which path loss between two known/matched antennas is characterized, and then the transmitting antenna is replaced by the unknown antenna.

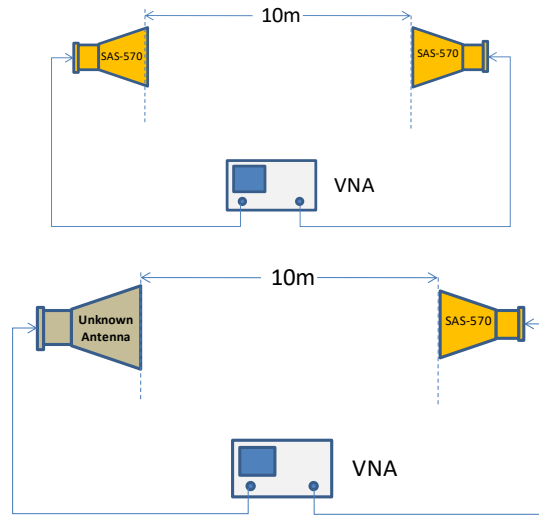


Figure 9 Two-antenna method for determining gain

Assuming the two SAS-570's are nearly identical antennas whose polarizations are matched, and placed at a known distance apart; the Friis Transmission Equation [REF7] can be used to determine the path loss between the two antennas.

$$(G_{tx})_{dB} = (G_{rx})_{dB} = \frac{1}{2} \left[20 \log\left(\frac{4\pi R}{\lambda}\right) + 10 \log\left(\frac{P_r}{P_t}\right) \right]$$

Where,

$$R = 10\text{m}$$

$$\lambda = \frac{c}{f_{\text{lower}}} \rightarrow \frac{c}{f_{\text{upper}}}$$

$$20 \log\left(\frac{4\pi R}{\lambda}\right) = \text{Path Loss}$$

$$10 \log\left(\frac{P_r}{P_t}\right) = \text{S21}$$

With the path loss now known, the gain of the unknown antenna can be determined as follows:

$$(G_X)_{dB} + (G_{AH})_{dB} = 20 \log\left(\frac{4\pi R}{\lambda}\right) + 10 \log\left(\frac{P_r}{P_t}\right),$$

solving for G_X :

$$(G_X)_{dB} = PathLoss + S21 - (G_{AH})_{dB}$$

2.2 Prodyn Free-Field Electric Field Sensor

The most common sensor used by APELC for radiated measurements is the Prodyn free-field, electric field sensor. This type of sensor can be generally characterized as a “D-dot” probe, in that it measures the first time derivative of the electric field displacement vector, and is described by the following relationship:

$$V_o = A_{eq} \frac{dD}{dt} R$$

The above equation states that the output voltage for the sensor (V_o) is the product of the probe effective area, the first time derivative of the electric field ($\frac{dD}{dt}$), and the impedance of the output circuit (R) [REF3]. Therefore, to obtain the electric field, D must be solved for and then divided by the permittivity of free space. The integration required in this operation is typically performed numerically, either as a math function on the recording oscilloscope, or in post by another piece of software such as LabVIEW™, MathCAD™ or Excel™.

This specific type of D-dot probe is also known as an asymptotic conical dipole [REF8], and utilizes dual capacitive sensing elements, placed 180 degrees apart to measure vertically, or horizontally polarized electric fields [REF3]. The two sensing elements share a common ground plane and can be fed directly into a balun to combine the two signals, and provide a single, unbalanced, 50-Ohm output (Figure 10). The addition of the two equal and opposite signals provides the benefit of cancelling any common-mode noise present on the probe.



Figure 10 Prodyn AD-55 Free-field electric field sensor and BIB-100F balun

Although APELC has used other Prodyn D-dot probes in the past, the model AD-55 has become the most common, due to its larger equivalent area, which provides a higher signal level compared to smaller models. This ensures that the signal, while still low enough to not cause electrical breakdown of the cabling, is high enough to be substantially above any noise generated by the source. Other considerations which make the probe a good fit for most APELC testing is its 2-GHz frequency response, and the fact that many of the Department of Defense facilities APELC collaborates with also use a similar if not identical probe. Additional specifications for the probe and balun are outlined in Table 2 and Table 3.

Table 2 AD-55 Specifications

<i>AD-55 D-dot Sensor</i>		
<i>Equivalent Area</i>	3X10 ⁻³	m ²
<i>Frequency Response (3dB pt.)</i>	2	GHz
<i>Risetime (10-90%)</i>	<.17	ns
<i>Maximum Output</i>	+/- 1.5	kV
<i>Output Connector</i>	SMA (Male)	

Table 3 BIB-100F Specifications

<i>BIB-100F Balun</i>		
<i>Bandwidth</i>	.0002-3.5	GHz
<i>Insertion Loss</i>	8	dB
<i>Propagation Delay</i>	0.6	ns
<i>Max Input Voltage</i>	1	kV
<i>CMMR</i>	28	dB
<i>Port Impedance</i>	50	Ohms

While calibration of the balun is conducted using a Vector Network Analyzer (VNA), the D-dot probe is solely calibrated by an accurate and NIST (National Institute of Standards and Technology) traceable measurement and verification of its equivalent area. As the sensor's transfer function is directly related to its mechanical dimensions by Maxwell's equations, this serves as the only required means of verifying the probe's sensitivity. Therefore, so long as the probe remains mechanically intact, no periodic calibrations are required due to the fact that no degradable components are present in the sensor [REF3].

3. Cabling

Coaxial cabling provides the link between the previously mentioned probes and the recording equipment. As a result, it is critical the cabling used be low-loss, mechanically robust, and shielded against noise present on the test range.

Table 4 Comparison of cabling used at APELC for radiated measurements

Cable	<i>RG-400</i>	<i>RG-214</i>	<i>Micro-Coax</i>
Attenuation/100 ft @ 1 GHz	13 dB	9 dB	15 dB
Shielding	Double	Double	Double
Impedance	50 Ohms	50 Ohms	50 Ohms
Connector	SMA	N-Type	SMA
Max Dielectric Voltage (RMS)	1900	5000	5000
Useage	Non-radiated signals (voltage & current)	Radiated Signal measurement	Radiated Signal measurement

Three major types of cabling are used by APELC, and are characterized and compared in Table 4. The first, RG-400, is a double-shielded 50-Ohm cable used for non-radiated measurements (e.g. voltage and current probes). While all the cabling used by APELC is double-shielded, the RG-400 provides the least shielding effectiveness of the three, and is therefore reserved for direct measurements where the measured signal is directly ground-referenced from the source to the scope. The coaxial cable is typically purchased in bulk, and connectorized in-house depending on the application (most often SMA).

RG-214 is an extremely versatile coaxial cable good for both transmission of high-voltage pulses, and receiving of pulsed and CW signals. Due to its heavier gauge center-conductor, RG-214 is both low-loss and mechanically robust. Furthermore, with an excellent shielding effectiveness, RG-214 is capable of measuring radiated signals with little effect from noise coupling onto the shield.

The third type of coaxial cabling used by APELC is the Micro-Coax brand, model UFA147B. This cable was first used at APELC when it was discovered that noise coupling onto the cable used for measuring the pulse in a MIL-STD 461G, RS-105 test platform (Figure 11) was introducing a considerable offset onto the resultant waveform. A Prodyn AD-55 D-dot probe is placed in the center of the RS-105 test volume, and as a result, the cabling connecting the probe to the oscilloscope is subjected to the 50 kV/m electric field generated by the tester. Aside from taking precautions to keep the cabling perpendicular to the electric field, the exceptional shielding on the Micro-coax cable helped to ensure that the signal integrity was maintained.



Figure 11 APELC MIL-STD 461G RS-105 Test Platform for 2m EUT's

In systems where extremely long cable runs create the opportunity for common-mode noise coupling that can interfere with the measurement, APELC utilizes optical links such as the PPM G-series link shown in Figure 12. These analog optical links replace long-runs of coaxial with optical fiber, thereby eliminating the coupling path for the high-power, transient RF environment inherent in these types of tests.



Figure 12 PPM G-series optical link transmitter

4. Calibration

All cabling and attenuators used at APELC are verified and calibrated using a Vector Network Analyzer (Figure 13). The device being tested is placed between the two ports of the VNA, and an S21 measurement is recorded. This measurement provides the insertion loss for the cables and attenuators, which is then kept in a hard and soft-copy log for reference by the test engineer. Calibration of the VNA is conducted with a NIST-certified Electronic-calibration (Ecal) module [REF9]. The Ecal unit provides the VNA with a set of standards for short-circuit, open-circuit, and broad-band 50-Ohms loads, so that each measurement taken with the VNA is NIST-traceable.



Figure 13 VNA measurement of diagnostic cabling

5. Acquisition

Acquisition of radiated signals at APELC is performed using one of several Tektronix oscilloscopes, depending on the resolution needed to capture the frequency content of the signal. The most commonly used instrument is the Tektronix DPO-7254 (Figure 14), which has a 2.5 GHz bandwidth and 40 GS/s of sampling resolution. For the higher frequency signals produced by APELC HPM devices, a TDS-6604 oscilloscope is used, with 6 GHz bandwidth and 20 GS/s of resolution.

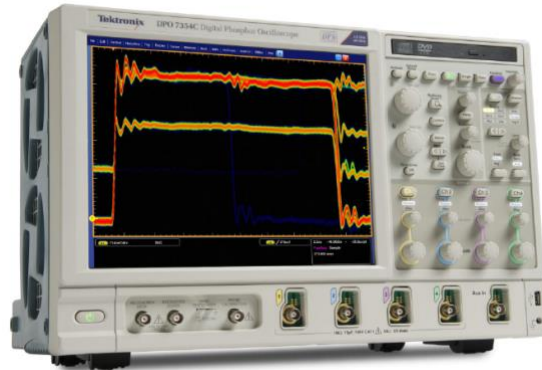


Figure 14 DPO 7254 Oscilloscope

Both previously mentioned oscilloscopes are equipped with GPIB (General Purpose Interface Bus), so that an external program can communicate with the oscilloscope. An example of this application is shown in Figure 15, in which a LabVIEW™ application was developed at APELC to acquire the raw data from a D-dot probe, recorded on an oscilloscope. As mentioned previously, the D-dot signal requires not only integration, but also scaling and offset removal to produce a representative waveform. Using the GPIB interface to communicate with the host oscilloscope, the program captures the raw spreadsheet data file (.csv), plots it on the screen, allows the operator to remove the offset and enter probe, cable, and attenuator specifications, and plots the scaled waveform. The plot can then be saved to a spreadsheet file for later use.

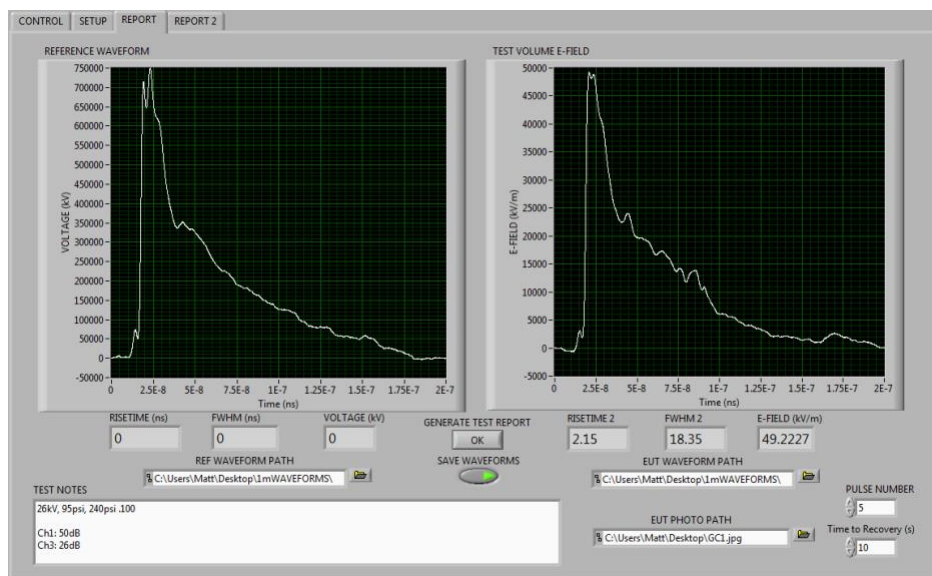


Figure 15 LabVIEW data acquisition software for D-dot measurements

Because a wideband or UWB signal has a wide bandwidth, picking a single frequency for attenuation does not provide as accurate of a result compared to finding the attenuation across the signal's bandwidth. More recently, APELC has begun employing Voss Scientific DAAAC acquisition software, allowing us to correct attenuation for frequency across the entire spectrum of the signal. An S21 measurement (taken using a VNA- See the "Calibration" section of this document) of the signal chain is entered into the software, which then auto-correlates this with the FFT of the signal to yield accurate scaling for the waveform.

6. Typical Measurement

An example of a typical 10-meter test range measurement is provided in the form of a Factory Acceptance Test (FAT) for a previous customer. In this particular instance, the device being tested was a 60-MHz dipole with an integrated resonator. An APELC MG15-3C-940PF Marx generator sourced the dipole, and measurements were made using the Prodyn AD-55 D-dot probe. The test range is shown in Figure 16.



Figure 16 10-meter range testing of a 60-MHz dipole.

A 100-meter section of RG-214 cabling provides the link between the AD-55 D-dot probe and the exterior bulkhead shown in Figure 17. On the interior of the building, a second set of cabling connects the bulkhead to the screen-room pictured in Figure 18. The screen room was originally manufactured by ETS Lindgren, and provides filtered AC power entry and over 80-dB of shielding effectiveness.



Figure 17 Test-range bulkhead



Figure 18 APELC screen room

The data was then collected on a Tektronix DPO-7254 oscilloscope and processed using an Excel™ worksheet to integrate, remove offset, and scale the raw signal from the D-dot probe. Figure 19 shows the completed FAT document provided to the customer, showing the test set-up, peak electric field, standard deviation, and FFT.

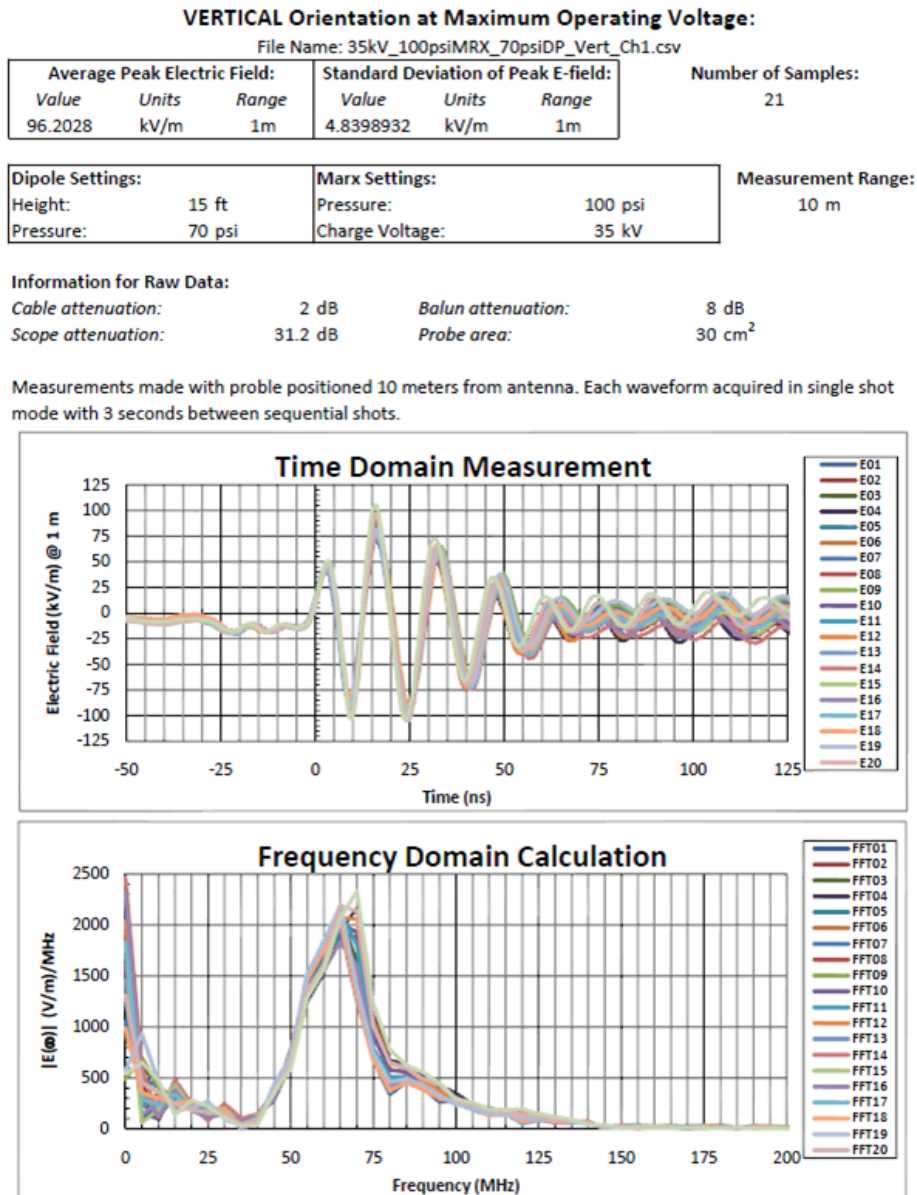


Figure 19 Factory Acceptance Test example worksheet

7. Conclusion

APELC utilizes a complete suite of sensors, antennas, oscilloscopes and other diagnostic tools to acquire and process the signals generated by high-power RF sources. The knowledge-base and associated hardware at APELC allow for the characterization of Ultra-wideband, Wideband, and Narrowband sources.

REFERENCES

- 1.) Taylor, James D., ed. *Introduction to ultra-wideband radar systems*. CRC, 1994.
- 2.) Mayes, J. R., and W. J. Carey. "The generation of high electric field strength RF energy using Marx generators." *Power Modulator Symposium, 2002 and 2002 High-Voltage Workshop. Conference Record of the Twenty-Fifth International*. IEEE, 2002.
- 3.) W.R. Edgel, Primer on electromagnetic field measurements, Prodyn Application Note 895, Prodyn Technologies (www.prodyntech.com)
- 4.) Benford, James, John A. Swegle, and Edl Schamiloglu. *High power microwaves*. Taylor & Francis, 2007.
- 5.) J. D. Kraus. *Antennas*, 2nd edition, *McGraw-Hill*. New York, 1988
- 6.) http://www.ahsystems.com/Datasheets/SAS-570_Horn_Antenna_Datasheet.pdf
- 7.) Balanis, C. A., *Antenna theory: analysis and design*. J. Wiley, New York, 1982.
- 8.) C. E. Baum, "Sensors for Measurement of Intense Electromagnetic Pulses," in *Proc. 3rd IEEE Int Pulsed Power Conf.*, 1981, pp. 179–185.
- 9.) <http://www.home.agilent.com/agilent/product.jsp?nid=-35190.536905582.00&lc=eng&cc=US>